Ultrapyrolysis of Propane in a Spouted-Bed Reactor with a Draft Tube

Ultrapyrolysis or ultrarapid pyrolysis is a hydrocarbon thermal cracking process which offers the promise of greater product selectivity, higher yield and feedstock flexibility. In this paper, ultrapyrolysis of propane in a spouted bed with a draft tube was used as a test system to demonstrate these advantages. Experiments, carried out on a 20-cm-diameter pilot-scale reactor, illustrate the spouted bed to be capable of achieving the extremely high reactant heating rates of up to 10^5 K/s and the short gas residence times of less than 500 ms necessary for this process. Moreover, reactant conversion and product yields can be enhanced by controlling the operating temperature of the bed. In addition, application of the propane pryolysis reaction scheme of Sundaram and Froment into a recently developed computer model indicates the ability to correctly simulate the spouted bed as an ultrapyrolysis reactor.

Rudolf K. Stocker
John H. Eng
William Y. Svrcek
Leo A. Behie
Department of Chemical and Petroleum Engineering
University of Calgary
Calgary, Alberta, Canada T2N 1N4

Introduction

Thermal pryolysis has applications not only in olefins production, but also in other applications of great significance. The world supply of conventional crude oil, for instance, is in rapid decline (Bailey, 1984). There exist relatively abundant supplies of heavy crude oils, tar sands bitumens, and refinery vacuum residues, but current processes for conversion of these heavy feedstocks to the lighter weight hydrocarbons required as fuels and chemical precursors suffer from a combination of low yield, limited flexibility with regard to feedstock variability, limited product selectivity, and deleterious environmental side-effects. Ultrapyrolysis or ultrarapid pyrolysis, which is typified by temperatures in excess of 700°C and reactant residence times much less than 500 ms, offers the promise of improvement in some or all of these areas, in particular with regard to feedstock flexibility, and product selectivity and yield. This has been clearly demonstrated by the pioneering work of Bergougnou and his coworkers (Berg et al., 1986). Furthermore, recent industry advances have been reported such as the quick contact (QC) reaction system of the Stone and Webster Eng. Corp. (Gartside, 1989) and the ART process of the Engleland Corp. (Geren and Center, 1985).

The thermal pyrolysis of hydrocarbons in general and lighter hydrocarbons in particular can be characterized as a set of fragmentation and recombination reactions which occur in series-parallel order. Any given reaction, in accordance with the generally-accepted free-radical chain initiation, propagation and termination mechanisms, produces either final product or feedstock for further reaction. The two major parallel reaction pathways competing for the feedstock, however, are the (desirable) hydrocarbon recombination reactions, which result in products of interest, and the (undesirable) coking reactions, which yield carbon from lighter hydrocarbons and highly naphthenic structures from heavier hydrocarbons.

As a result of the parallel nature of the product yielding and coking reactions, any hydrocarbon thermal cracking process constitutes an economic balance between feedstock sacrificed to byproduct coke and the measures necessary to minimize the loss.

Spouted beds have been applied in operations as diverse as grain drying, solids coating, and heavy oil pyrolysis (Mathur and Epstein, 1974). Naturally, because homogeneous and especially vapor-phase chemical reactions are of great commercial importance, considerable attention has been paid to spouted bed chemical reactors over the years. A brief description of the gas-solid interactions involved in spouted-bed operation can elucidate the beneficial features of these beds as chemical reactors.

Spouting results from the introduction of a fluid at a single orifice in the bottom of a bed of granular solids. If the solids within the bed are sufficiently large (>1 mm diameter) and if

Correspondence concerning this paper should be addressed to L. A. Behie.

the bed height is below a certain maximum value, the fluid clears a passage up through the bed and the bed is said to be "spouting." In passing through the bed, the fluid entrains granular solid material which is carried up the spout with it. On emerging from the top of the bed, the fluid jet diverges and its capacity for transporting the entrained solids is considerably reduced. These solids thus form a fountain and rain out over and settle on top of the annular bed around the spout, which continues to exist where the original bed was. Hence, a solid circulation pattern is established. If a solid draft tube—a vertically-aligned tube which serves to contain the spout—is included in the bed, the spout effectively becomes a vertical transport riser. The major advantage of this is the reduction of spout gas divergence or bypassing into the annulus resulting in both narrower gas residence time distributions and successful operation at bed depths much greater than the maximum spoutable depth of conventional beds.

Due to the fluid-solid interactions accompanying spouted-bed operation, its advantages in terms of use as a chemical reactor lie not as a catalytic reactor, but as a gas-phase reactor with bed particles acting as heat sources. In this capacity, residence times of entering gas can be kept quite low. In addition, it will be demonstrated that a spouted bed can heat the spout gases at the extremely high rates necessary for ultrarapid pyrolysis. It will also be shown that a draft tube offers further advantages by limiting divergence of the spout gases into the annulus, thus allowing better control over the contact time of the entering gases. Moreover, we have succeeded in ultrapyrolyzing steam-atomized Alberta heavy oil at 1.0 bbl/d (159 L/d) in a spouted bed with a draft tube to produce an upgraded oil of low viscosity (280 mPa · s at 25°C).

The intent behind this research was to demonstrate that ultrarapid pyrolysis (ultrapyrolysis) can be successfully carried out in a spouted bed with a draft tube and to validate a recently-developed nonisothermal spouted-bed reactor computer model (Stocker, 1987; Stocker et al., 1989).

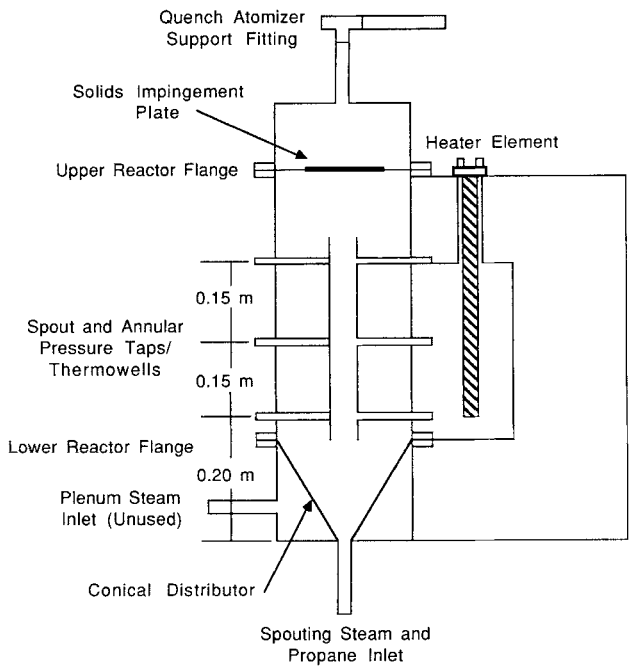

Figure 1. Side view of conic-base cylindrical pilot-scale steam-spouted-bed reactor and reactor heating furnace.

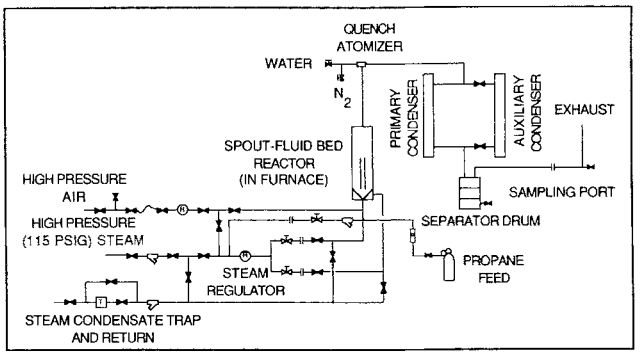

Figure 2. Propane pyrolysis experiments in conic-base, pilot-scale, cylindrical reactor spouted with steam.

Experimental Studies

A large, pilot-scale (20.0-cm) test bed was built to conduct the pyrolysis experiments. The bed was fully round and was enclosed in a custom-built clamshell furnace capable of reaching temperatures of 1,200°C, with total bed height 165 cm from inlet nozzle to exhaust. Figure 1 illustrates the bed's design in a sectional view. Figure 2 is a schematic flow diagram of the pilot plant. Bed dimensions are summarized in Table 1. The reactor was made of Monel alloy 410 metal and fabricated in three separate sections. The base of the bed was a conic grid plate (60° included angle) over a plenum chamber (the bed was designed so that it could operate as a spout-fluid bed) with a centrally-located inlet nozzle of 2.54 cm ID. The upper flange of this section was flush with the top of the cone. The middle section was cylindrical and contained a centrally-located draft tube (4.0 cm ID, of approximately circular cross-section, and 0.60 m total length). Both the bed wall and the draft tube were fabricated of rolled and welded 1.52 mm (U.S. Standard 16 gauge) sheet Monel 410. The draft tube was fixed at a single position by 12 radial tubing supports, spaced at right angles to one another at three levels, 15 cm apart. The draft tube supports, of 0.635 cm OD [¼ in. (6.4 mm) nom] tubing, also served as thermowells and pressure taps. Of the 12 supports, six were drilled through to the interior of the draft tube. The other six were perforated vertically about the midpoint of the annulus, but closed off from the spout. The supports were extended approximately 2 cm to the exterior of the bed. Tubing fittings connected those tubing supports serving as pressure taps to lines leading down through the

Table 1. Principal Geometric Variables of Pilot-Scale Conic-Base Cylindrical Steam-Spouted Bed Reactor

Variable	Value
Inlet diameter (D_i)	0.0254 m
Draft tube diameter (D_t)	0.04 m
Column diameter (D_c)	0.20 m
Length of entrainment region (L_e)	0.151 m
Length of conic region (L_c)	0.151 m
Length of draft tube (L_t)	0.60 m
Length of disengaging zone (L_d)	0.868 m
Included cone angle (θ)	60°

bottom of the furnace. Chromel-alumel (K-type) thermocouples were inserted through the remaining supports. Annular thermocouples extended to the midpoint of the annulus. Spout thermocouples were inserted into the spout to a depth of 0.5 cm. The top section of the bed was a flanged cap supporting the overhead exhaust line and a flat, centrally-positioned, 10-cm-diameter breaker plate to reduce the amount of solids carryover.

The bed was spouted with steam from the building steam supply. A regulator was used to reduce the steam pressure to less than 170 kPa. Calibrated plate orifices in the supply lines were used to measure inlet steam flow rates. A removable air supply line was also provided to permit testing with air as the spouting fluid.

Process heat was supplied by a custom-built clamshell furnace which surrounded the reactor. A total of 12 bayonet-type silicon-carbide heating elements were vertically arrayed in a circular arrangement about the reactor, at a distance of approximately 6 to 8 cm from the bed walls. A 20-cm-thick cylindrical lining of Durablanket 2600 high-temperature refractory insulation surrounded the elements and reactor hot zone. Furnace power was supplied by a pair of multitap step-up transformers rated from 260- to 600-V AC and a maximum power of 30 kW each. Power levels were controlled with a Rex C-1000 microprocessor-based temperature controller with self-tuning, PID algorithm parameter setting, and control capability. The power supply and controller were purchased as a unit from Pyradia Inc., Longueuil, Quebec.

The reactant feed used was Matheson-Instrument-grade propane with a nominal purity of 99.5%. A GC analysis of the feed propane composition revealed it to be 99.84% pure. Propane was supplied for the pyrolysis tests from a bottle and regulator through a Matheson 604 rotameter. It was fed to the reactor through a tap on the spouting gas inlet line. Exhaust gases exited the bed via a heavily-insulated exhaust line and were quenched by direct contact with an atomized nitrogen-water spray injected cocurrently with the reactor effluent flow. Thermocouples were placed up and downstream of the atomizer location to monitor the effectiveness of the quench. Additional cooling was provided by the product condensers, which recovered most of the steam. Noncondensable gases were exhausted to the atmosphere through an orifice meter. Exhaust gas samples were drawn from a tap on this line through a desiccant bed and into a glass sample bomb with an aspirator bulb.

Temperature measurement

The spouted bed itself was instrumented with six K-type thermocouples, located as described in the preceding section. The thermocouples were obtained with long (0.914-m) Inconel sheaths to protect them within the high-temperature zone. Others were located adjacent to the inlet flow orifices in the exhaust line 0.1 m upstream and 0.3 m and 0.5 m downstream of the quench atomizer, and in the inlets and outlets of the product condensers. A total of 26 thermocouples were used to measure temperatures at various points of the plant. This array was connected to the Taurus One data logger and a Compaq 286 portable microcomputer. The data logger scanned the array sequentially on receipt of a trigger signal from the computer. Analog thermocouple output signals were digitized and linearized, with automatic cold-junction temperature compensation, by the Taurus. The linearized temperature reading (in engineering units) was then transmitted back to the computer, where it was stored, with the elapsed time from the start of logging, to a disk file and readings from the entire array were displayed on screen. Employing a custom data logging program written in compiled BASIC, the data logging system was capable of up to 20 scans per minute, including the overhead due to multiple scans of the differential pressure signals, flow rate computations, and processing and display of data.

Unit operation

As this unit was capable of achieving steady-state temperatures of 900°C, while spouting, little difficulty was encountered in obtaining a continuous pyrolysis gas sample. The bed, filled to the level of the top of the draft tube (75 cm above the level of the inlet nozzle) with round silica sand ($\bar{d}_p$ = 1.03 mm, sphericity ≈ 1.0) was spouted initially with air and the furnace turned on until the bed reached a temperature of 200°C. At that point, the steam lines were "blown down"—flushed to condensate recycle for a period of 10 to 15 minutes at moderate flow rates, in order to bring the steam lines to operating temperature. The bed was then spouted with steam and the furnace controller set-point temperature set to the desired reactor wall temperature. There was always some initial overshoot of the target temperature (typically 50°C), but furnace temperature fluctuations were generally 20°C or less. Steady state was assumed reached once the spout temperature was observed to fluctuate both negatively and positively on successive readings by the data-logging program. At that point, the propane feed lines were flushed with nitrogen and an approximate feed rate set on the propane feed rotameter. Propane feed into the reactor was then started. After 10 minutes of continuous pyrolysis, a gas sample was taken as described below. Conditions for a set of pyrolysis experiments are described in Table 2.

Some difficulty was encountered with merely determining whether or not the bed was spouting normally at high temperatures. Difficulties were also encountered with sand fines and steam incursions into the pressure lines, despite the use of a continuous nitrogen backflush on each tap to prevent this. This problem made comparison of the regional axial pressure gradients unreliable for any of the high-temperature tests, although this method had worked well when the spouting fluid was air. Ultimately, the method evolved was to force a step change in the furnace set-point temperature and monitor the dynamic response of the thermocouple readings from the two regions of the bed. When the spout wandered outside the draft tube, the annular temperatures still changed rapidly, but the spout thermocou-

Table 2. Pilot-Scale, Conic-Base, Cylindrical, Spouted-Bed Reactor Propane Pyrolysis Experiment*

Experiment	1	2	3
Spouting gas flow rate (kg/s)	1.0×10^{-2}	1.0×10^{-2}	1.0×10^{-2}
Propane flow rate (kg/s)	6.8×10^{-4}	6.8×10^{-4}	6.8×10^{-4}
Inlet reactant conc. (mol/m^3)	1.09×10^{-3}	1.09×10^{-3}	1.09×10^{-3}
Furnace temp. (K)	1,270.0	1,326.0	1,390.0
Exhaust gas temp. (K)	978.0	1,051.0	1,138.0
Sample time (elapsed min)	10.0	8.0	11.0

*Bed material, silica sand
Particle diameter (mm), 1.03
Annular bed depth (m), 0.75
Spouting gas, steam

ple readings lagged well behind. When the bed was not spouting at all, bed temperatures varied sluggishly and the furnace-bed temperature differential was much larger than for normal spouting operation.

Gas analysis

All exhaust gas samples taken during experimental runs were analyzed by gas chromatography. The analysis was carried out on an HP-5830A gas chromatograph using a TCD detector at 300°C. Columns used were a 3.2-mm (⅛-in.)-diameter, 0.914-m-long Poropak Q column, switching to a 3.2-mm (⅛-in.)-diameter, 0.914-m-long mole sieve 13X. The GC was temperature-programmed to start at 50°C and hold this for 11 minutes, then ramp increase to 200°C at 30°C/min and hold there to the end of the analysis at the 20-minute mark. Helium at 30 mL/min was used as the carrier gas.

Gas samples from the runs were also reanalyzed to evaluate a new chromatographic column and method on a Varian Vista 6000 with a TCD detector at 240°C. The temperature of the 3.2-mm (⅛-in.)-diameter, 3.05-m-long Poropak QS column was programmed to hold at −20°C for 1 minute initially, then ramp increase at 20°C/min to 230°C and hold there for 3 minutes to run termination. Helium at 20 mL/min was used as the carrier gas.

Steady-State Model

Predictions from a computer simulation developed by Stocker (Stocker et al., 1986; Stocker, 1987; Stocker et al., 1989) were compared with the experimental results obtained. The computer simulation was derived to evaluate the feasibility of employing a spouted-bed reactor with a draft tube for fast, multiple reactions such as those encountered in propane pyrolysis. Propane pyrolysis was specifically used as the test reaction due to the large amount of literature available regarding its reaction kinetics and reaction products.

The mass, momentum and energy flow characteristics in the bed were simulated by separately analyzing the effects in the annulus, spout, and fountain regions, while accounting for the applicable interactions between these three regions. Flows of solids and gaseous components were accounted for by development of material balance equations.

Spout region

Derivation of the material balance equations for the solids and gases within the spout result in the following equations for the spout voidage and gas velocity, respectively:

$$\frac{d\epsilon_s}{dz} = (1 - \epsilon_s)\left[\frac{dv_s/dz}{v_s} + \frac{dA_{cs}/dz}{A_{cs}} - \frac{dW_s/dz}{W_s}\right] \quad (1)$$

and

$$\frac{du_s}{dz} = -u_s\left[\frac{d\epsilon_s/dz}{\epsilon_s} + \frac{d\rho_{gs}/dz}{\rho_{gs}} + \frac{dA_{cs}/dz}{A_{cs}} - \frac{dG_s/dz}{G_s}\right] \quad (2)$$

Similarly, a balance on the momentum of solids and gases within the spout at any given height yields the following equations for spout particle velocity and axial spout pressure, respectively:

$$\frac{dv_s}{dz} = \frac{(v_{so} - v_s)}{W_s}\frac{dW_s}{dz} + \frac{3C_D\rho_{gs}(u_s - v_s)}{4d_p\rho_p v_s}|u_s - v_s| + \frac{g}{v_s}\left[\frac{\rho_{gs}}{\rho_p} - 1\right] - \frac{1}{\rho_p v_s}\frac{dP_s}{dz} - \frac{2v_s}{D_s}f_{pw} \quad (3)$$

and

$$\frac{dP_s}{dz} = \frac{-u_s}{\epsilon_s A_{cs}}\frac{dG_s}{dz} - \rho_{gs}u_s\frac{du_s}{dz} - \frac{3(1 - \epsilon_s)C_D}{4\epsilon_s d_p} \cdot \rho_{gs}(u_s - v_s)|u_s - v_s| + \frac{(1 - \epsilon_s)}{\epsilon}g(\rho_{gs} - \rho_p) - g\rho_{gs} - \frac{2\rho_{gs}u_s^2}{D}f_{gw} \quad (4)$$

Annular region

The physical exchange of particles between the spout and the annulus necessitates the incorporation of a function to describe the solids circulation rate:

$$\frac{dW_a}{dz} = \frac{W}{L_e} \quad (5)$$

While Berruti et al. (1988) have studied the solids circulation in a particular configuration of a cold, semicylindrical, spout-fluid bed, the scarce amount of information available regarding solids circulation in a high-temperature bed required that the solids circulation rate be varied to match observed spout temperature profiles. Similar accounting for the gas divergence from the spout to the annulus results in the following equations:

$$\frac{dG_a}{dz} = G_a\left[\frac{du_a/dz}{u_a} + \frac{d\rho_{ga}/dz}{\rho_{ga}} + \frac{dA_{ca}/dz}{A_{ca}}\right] \quad (6)$$

and

$$\frac{dG_s}{dz} = -\frac{dG_a}{dz} \quad (7)$$

where the annular gas velocity is calculated by employing a modified version of the Mamuro-Hattori equation (Mathur and Epstein, 1974).

The annular pressure gradient is computed assuming Darcy-type flow in the annulus:

$$\frac{dP_a}{dz} = -K_a u_a \quad (8)$$

and incorporating the Blake-Kozeny equation in calculating the value of the proportionality constant K_a.

Fountain region

The fountain is treated simply as an expanding, decelerating, two-phase jet—the spout stream emerging from the top of the

draft tube and mingling with a compressing, accelerating, surrounding medium, and the gases emerging from the annulus (Stocker, 1987).

Thermal energy equations

Thermal energy balances can be written for the individual flowing phases in each of the regions to describe heat transfer within the bed. The energy balance for the annular solids results in an explicit differential relation for the second derivative of the solids temperature:

$$\frac{d^2T_{pa}}{dz^2} = \left[\frac{W_a C_{p_p}}{k_{ea}A_{ca}} - \frac{\frac{dA_{ca}}{dz}}{A_{ca}}\right]\frac{dT_{pa}}{dz} - \frac{\pi D_c}{k_{ea}A_{ca}}\left[h_w(T_w - T_{pa}) + \sigma F_{wa}(T_w^4 - T_{pa}^4)\right] + \frac{\pi D_s}{k_{ea}A_{ca}}\left[U_t(T_{pa} - T_{gs}) + \sigma F_{tp}(T_{pa}^4 - T_{ps}^4)\right] + \frac{6(1-\epsilon_a)h_{pa}}{k_{ea}d_p}(T_{pa} - T_{ga}) \quad (9)$$

Energy balances for the flowing phases in the spout yield relationships for the spout solids and gas temperatures, respectively:

$$\frac{dT_{ps}}{dz} = \frac{(T_{pa} - T_{ps})}{W_s}\frac{dW_s}{dz} - \frac{6\sigma F_{pt}}{\rho_p v_s C_{p_p} d_p}(T_{ps}^4 - T_{pa}^4) - \frac{6h_{ps}}{\rho_p v_s C_{p_p} d_p}(T_{ps} - T_{gs}) \quad (10)$$

and

$$\frac{dT_{gs}}{dz} = \frac{6h_{ps}(1-\epsilon_s)}{\rho_{gs}u_s C_{p_{gs}} d_p}(T_{ps} - T_{gs}) + \frac{\pi D_s U_t}{G_s C_{p_{gs}}}(T_{pa} - T_{gs}) - \frac{\Delta Hr_s}{C_{p_{gs}}\rho_{gs}u_s} \quad (11)$$

Assuming thermal equilibrium of the solids and gases within the fountain region (an assumption substantiated by model predictions) implies that the only remaining energy sink in the fountain region is caused by the on-going gas-phase reaction:

$$\frac{dT_{gs}}{dz} = \frac{-\Delta Hr_s}{C_{p_{gs}}\rho_{gs}u_s} \quad (12)$$

and

$$\frac{dT_{ga}}{dz} = \frac{-\Delta Hr_a}{C_{p_{ga}}\rho_{ga}u_a} \quad (13)$$

Further details of the computer model are included in Stocker (1987) and Stocker et al. (1989).

Kinetic rate equations

The kinetics of the pyrolysis of propane for short reaction times have been extensively studied by Froment and coworkers (Van Damme et al., 1975; Froment et al., 1976; Sundaram and Froment, 1977, 1979; Sundaram et al., 1981). The pyrolysis mechanism which they proposed consists of 11 series and parallel reactions, including three reversible reactions, producing a number of product species from the intermediary products of other reactions as well as from the feedstock. The reaction rates were modeled with simple, low-order rate equations:

$$r_{ij} = K_{ij}[C_{mj}][C_{nj}] \quad (14)$$

with an Arrhenius-type temperature dependency:

$$K_{ij} = A_i e^{(-E_{ai}/R_g T_{gj})} \quad (15)$$

where

r_{ij} = ith reaction in region j of the bed

A_i = preexponential factor

E_{ai} = activation energy

The values of these reaction model parameters, A_i, and E_{ai}, are obtained by fitting experimental data.

Table 3 gives values for the preexponential factors and activation energies for computing the reaction rate constants for the 11 reactions specified by Sundaram and Froment (1979). Since both the draft tube and particles provide a repository surface for

Table 3. Kinetic Rate Constants for Thermal Propane Pyrolysis Reaction Mechanism, Including Coking Reaction*

Reaction No.	Preexponential Factor s^{-1} or $m^3/mol \cdot s$*	Activation Energy kcal/mol	Equilibrium Constant Reversible Reactions
1	4.692×10^{10}	50,600	
2	5.888×10^{10}	51,290	$\exp[(-14,348/T_g) + 11.085]$
3	2.536×10^{13}*	59,060	
4	1.514×10^{11}	55,800	
5	1.423×10^{9}	45,500	
6	3.794×10^{11}	59,390	$\exp[(-15,011/T_g) + 9.700]$
7	5.553×10^{14}*	60,010	
8	4.652×10^{13}	65,200	$\exp[(-16,228/T_g) + 10.760]$
9	1.026×10^{12}*	41,260	
10	6.960×10^{7}	34,320	
11	8.992×10^{10}	74,970	

*Sundaram and Froment (1979)

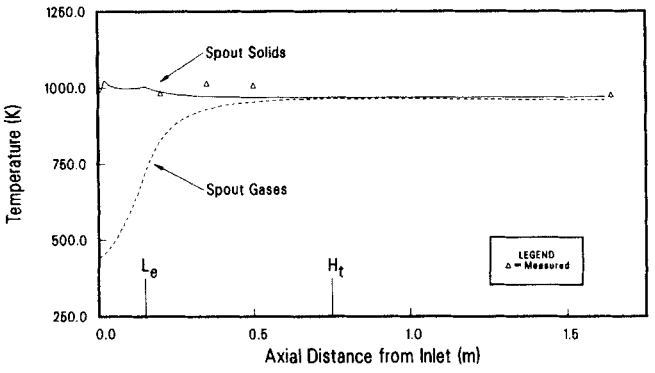

Figure 3. Pilot-scale reactor propane pyrolysis experiment 3: measured spout temperatures vs. simulated gas and solids spout temperature.

coke formation, the coke rate equation given by these authors was modified to take into account the additional surface.

Pyrolysis Tests

Axial temperature profiles

Axial temperature profiles were measured in the pilot-scale spouted-bed reactor during a series of pyrolysis tests. In modeling the reactor for the conditions of these tests, the solids circulation rate was varied to match the observed spout temperature profile, a justifiable modeling technique in view of the uncertainty associated with the predictions of published solids circulation rate correlations at high temperatures.

Figures 3 shows the axial spout temperature profiles for one of the tests in comparison with the best matched run from the simulation work. Figure 4 shows the axial annular temperature profiles for the same test. Since the solids circulation rate is adjusted in order to match the spout temperature profiles, the match between experimental and theoretical values is hardly surprising; however, Figure 3, in particular, illustrates both theoretically and experimentally that the heating rates within the spout are in fact extremely large as the spout gases quickly reach thermal equilibrium with the spout solids.

Product gas analyses

Table 4 presents the results of the analyses of gas samples taken during the tests mentioned. Figures 5 to 7 compare the

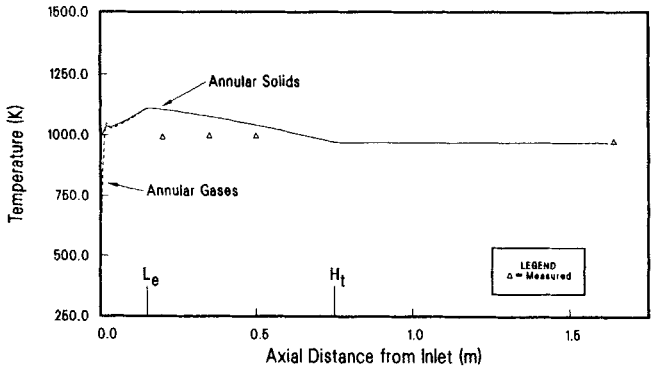

Figure 4. Pilot-scale reactor propane pyrolysis experiment 3: measured annular temperature vs. simulated gas and solids annular temperature.

Table 4. Dry Product Gas from Propane Pyrolysis Experiments in Pilot-Scale, Conic-Base, Cylindrical, Steam-Spouted-Bed Reactor on N_2/O_2-Free Basis

	Experiment No.		
Component	1	2	3
CO	—	—	0.0826
CO_2	0.0044	0.0189	0.0209
H_2	0.1076	0.1794	0.4267
CH_4	0.0824	0.0886	0.2213
C_2H_2	—	—	—
C_2H_4	0.0879	0.2071	0.2135
C_2H_6	0.0163	0.0077	0.0133
C_3H_6	0.0523	0.1134	0.0089
C_3H_8	0.6471	0.3639	0.0106
i-C_4 + n-C_4	0.0017	0.0210	0.0020
C_5+	—	—	—

results of analyses of gas samples taken during steady-state pyrolysis tests at three reactor temperatures with the predictions of the model for similar conditions. The accuracy of the predictions is outstanding. Product gas compositions predicted, which differ markedly for the various test temperatures, correspond very well to the analyses of the experimental gas samples. Propane conversion is predicted to be higher than found experimentally for the lower-temperature experiments—Figure 5 (720°C) and Figure 6 (790°C), but lower than experimentally determined at the highest temperature (880°C)—Figure 7. Furthermore, in general, material balances were closed within 10% in all our propane pyrolysis work.

Olefins production was maximized at the intermediate temperature of 790°C. Experimentation at the lowest temperature indicates the temperature to be sufficient to initiate the primary propane scission reaction. At the highest temperature, the shift to hydrogen and methane production is very apparent in both the product gas analysis and the simulation predictions. This indicates the trend towards primary product consumption and the formation of less desirable secondary products as cracking becomes excessively severe. In general, the trends indicate the necessity of accurate temperature control for maximum olefins production.

Reactor contact times

It is also important to note here than the Froment pyrolysis reaction mechanism was developed in part with product distri-

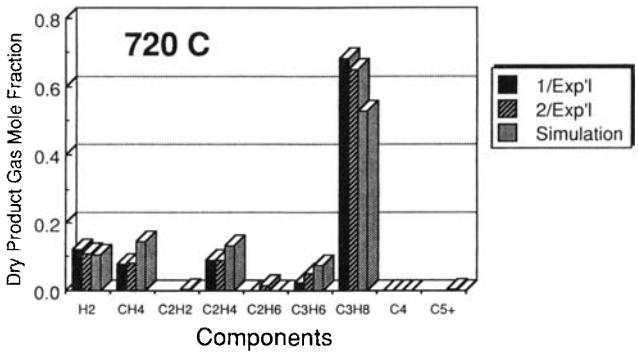

Figure 5. Pilot-scale propane pyrolysis experiment 1: predicted vs. measured hydrocarbon product distribution.

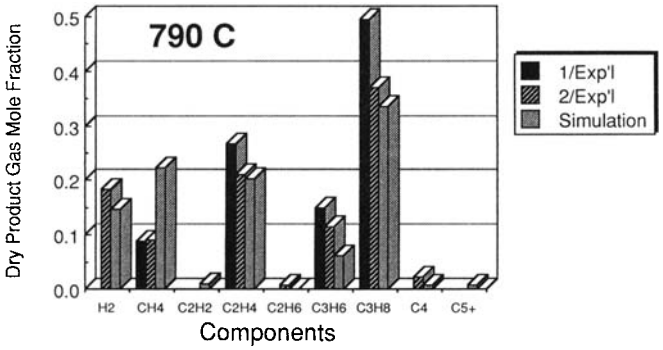

Figure 6. Pilot-scale propane pyrolysis experiment 2: predicted vs. measured hydrocarbon product distribution.

bution data from nonisothermal commercial-scale reactors with residence times in excess of 2.0 s. Table 5 compares actual residence times for gases in the spout and annulus computed in a simulation of the pilot-plant test. The model predicts that 17.8% of the inlet gas flow diverts to the annulus, with a total residence time in the reactor of 2.6 s. The remainder of the gas spends 430 ms in the reactor, a much shorter time than the cracking tube residence times of Sundaram and Froment. The fundamental correctness of their approach, despite their employment of the "equivalent reactor volume" concept (Hougen and Watson, 1947) in the analysis of their reactant conversion data, is demonstrated by the accuracy of predicted product distributions, even when extrapolated to much shorter reaction times, as demonstrated here.

Conclusions

This study has demonstrated that a spouted-bed reactor with a draft tube holds great promise as a reactor for fast, competing reactions such as hydrocarbons pyrolysis. The advantage to the use of a spouted-bed reactor with a draft tube have been shown to include very high reactant heating rates and extremely short gas residence times. Experiments were conducted in a pilot-scale reactor using propane pyrolysis to demonstrate these advantages, achieving high reactant conversions.

Results from this paper illustrate that spouted beds with a draft tube hold great promise for use as gas-phase chemical reactors, especially where gas residence time limitation is an

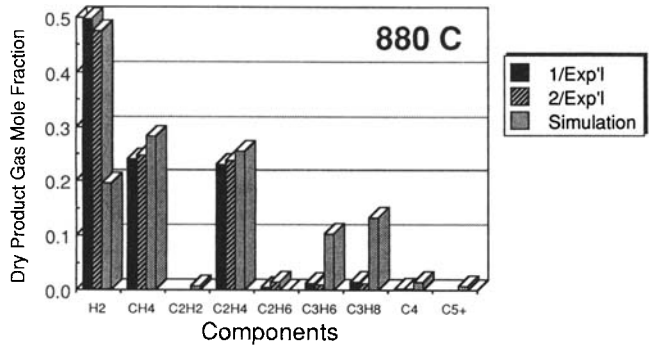

Figure 7. Pilot-scale propane pyrolysis experiment 3: predicted vs. measured hydrocarbon product distribution.

Table 5. Actual Residence Time in Spouted Bed for Experiment 3: Gas vs. Solids

Residence Time	Spout (s)	Annulus (s)
Gas (to H_t)	0.027	1.826
Gas (to exit)	0.431	2.608
Solids (to H_t)	0.287	229.7

important consideration, as in cases with fast, competitive reactions. Ultrapyrolysis of hydrocarbons, where the mean gas residence time at temperature must be kept to less than several hundred milliseconds, is a good example of a reaction for which the spouted-bed reactor with a draft tube is particularly suitable. Inclusion of the draft tube has been shown to greatly limit the total annular gas flow rate above the entrainment region compared with a conventional spouted bed—a feature essential to reducing the overall gas residence time in the spouted bed.

The propane pyrolysis reaction mechanism of Sundaram and Froment (1977, 1979) has been shown to match production distributions from pilot-scale experiments extremely well. This is encouraging because the use of their rate equations for such short reaction times is a significant extrapolation from the conditions for which their kinetic rate parameters were estimated.

Notation

A_c = cross-sectional area, m^2
A_i = pre-exponential factor for the ith reaction, L/s or $mol/m^3 \cdot s$
C_D = gas-particle drag coefficient
C_i = molar concentration of species i, mol/m^3
C_{mj} = concentration of species m in region j, mol/m^3
C_{nj} = concentration of species n in region j, mol/m^3
C_P = constant pressure specific heat, $J/kg \cdot K$
D_c = inside diameter of outer bed wall, m
D_i = inside diameter of inlet, m
D_s = spout diameter, m
D_t = draft tube diameter, m
d_p = mean particle diameter, m
E_{ai} = activation energy for ith reaction, $J/kg \cdot K$
F_{pt} = single particle-spout wall emissive view factor
F_{tp} = spout wall-solids emissive view factor
F_{wa} = wall-annulus emissive view factor
f_{gw} = gas-wall friction factor
f_{pw} = particle-wall friction factor
G_a = annular gas mass flowrate at height z, kg/s
G_s = spout gas mass flowrate at height z, kg/s
g = gravitational acceleration, $9.8087\ m/s^2$
ΔHr = composite heat of reaction including all reaction rate equations, $J/m^3 \cdot s$
h_p = particle-gas convective heat transfer coefficient, $W/m^2 \cdot K$
h_w = outer wall-annulus convective heat transfer coefficient, $W/m^2 \cdot K$
ID = inner diameter
K_a = Blake-Kozeny proportionality factor, $kg/m^3 \cdot s$
H_e = height of the draft tube entrance, m
H_t = height of top of draft tube, m
K_{ij} = reaction rate constant for the ith reaction in region j of the reactor, L/s or $mol/m^3 \cdot s$
k_{ea} = effective annular thermal conductivity, $W/m \cdot K$
L_c = length of basal conic region, m
L_d = length of disengaging zone, m
L_e = length of entrainment region, m
L_t = length of draft tube, m
P = pressure, Pa
r_{ij} = ith reaction in region j of the bed
R_g = universal gas constant, 8.3143 J/mol · K
T_g = gas temperature, K
T_p = solids temperature, K

T_w = bed wall temperature, K
U_t = draft tube overall convective heat transfer coefficient, $W/m^2 \cdot K$
u_a = axial annular gas velocity, m/s
u_s = axial spout gas velocity, m/s
v_s = axial spout solids velocity, m/s
W = total solids mass flowrate, kg/s
W_a = annular solids mass flowrate at height z, kg/s
W_s = spout solids mass flowrate at height z, kg/s
z = axial (vertical) distance from level of bed inlet, m

Greek letters

ϵ = voidage
ρ = density, kg/m^3
σ = Stefan-Boltzmann constant, $5.670\ 10^{-8}\ W/m^2 \cdot K^4$
θ = included basal cone angle

Subscripts

a = annulus
c = (outer) wall
g = gas
o = entering (from other region) or base value or outer
p = particle
s = spout
w = (outer) wall

Literature Cited

Bailey, R. T., "Opportunities and Challenges for Bitumen Upgrading Research," *Energy Proc./Canada,* (Sept.–Oct., 1984).

Berg, D. A., R. J. Summer, M. Meunier, C. L. Briens, and M. A. Bergougnou, "The Ultra-Rapid Fluidized (URF) Reactor, a Major New Reactor System," *Circulating Fluidized Bed Technology,* P. Basu, Ed., Pergamon Press (1986).

Berruti, F., J. R. Muir, and L. A. Behie, "Solids Circulation in a Spout-Fluid Bed With Draft Tube," *Can. J. Chem. Eng.,* **66,** 919 (1988).

Froment, G. F., B. O. Van de Steene, P. S. Van Damme, S. Narayanan, and A. G. Goosens, "Thermal Cracking of Ethane and Ethane-Propane Mixtures," *Ind. Eng. Chem. Proc. Des. Dev.,* **15,** 496 (1976).

Gartside, J. R., "QC—a New Reaction System," *Fluidization VI,* J. R. Grace, L. W. Shemilt, and M. A. Bergougnou, eds., Engineering Foundation, New York (1989).

Geren, P. M., and A. M. Center, "Upgrading and Enhanced Recovery of Tar Sand Bitumen and Heavy Crude using the ART Process," *Proc. Int. Conf. on Heavy Crude and Tar Sands/UNITAR,* Long Beach, CA (July 22–31, 1985).

Hougen, O. A., and K. M. Watson, *Chemical Process Principles,* **III,** Wiley, New York (1947).

Mathur, K. B., and N. Epstein, *Spouted Beds,* Academic Press, New York (1974).

Stocker, R. K., "Ultrapyrolysis of Propane in a Spouted Bed Reactor With a Draft Tube," PhD Thesis, Univ. of Calgary, Calgary (1987).

Stocker, R. K., J. H. Eng, and L. A. Behie, "Hydrodynamic and Thermal Modelling of a High Temperature Spouted Bed Reactor With a Draft Tube," *Can. J. Chem. Eng.,* in press (1989).

Stocker, R. K., A. Rastogi, L. A. Behie, W. Y. Svrcek, and M. A. Bergougnou, "A Computer Simulation of Propane Cracking in a Spout-Fluid Bed Reactor with a Draft Tube," *Fluidization V,* K. Ostergaard and A. Sorensen, eds., Engineering Foundation, New York (1986).

Sundaram, K. M., and G. F. Froment, "Modelling of Thermal Cracking Kinetics: I. Thermal Cracking of Ethane, Propane, and their Mixtures," *Chem. Eng. Sci.,* **32,** 601 (1977).

———, "Kinetics of Coke Deposition in the Thermal Cracking of Propane," *Chem. Eng. Sci.,* **34,** 635 (1979).

Sundaram, K. M., P. S. Van Damme, and G. F. Froment, "Coke Deposition in the Thermal Cracking of Ethane," *AIChE J.,* **27,** 946 (1981).

Van Damme, P. S., S. Narayanan, and G. F. Froment, "Thermal Cracking of Propane and Propane-Propylene Mixtures: Pilot Plant versus Industrial Data," *AIChE J.,* **21,** 1065 (1975).

Manuscript received Dec. 29, 1988, and revision received July 10, 1989.